An Anatomical Atlas-Based Method for fNIRS Imaging of the Rhesus Macaque

Yong Xu[1,2], **Tigran Gevorgyan**[1,3], **Douglas S. Pfeil**[1], **Daniel C. Lee**[1,3], **and Randall L. Barbour**[1,2]

[1] *SUNY Downstate Medical Center, 450 Clarkson Avenue, Box 25, Brooklyn, NY 11203*

[2] *NIRx Medical Technologies LLC, 15 Cherry Lane, Glen Head, NY 11545*

[3] *Interfaith Medical Center, 1545 Atlantic Avenue, Brooklyn, NY 11213*

yong.xu@downstate.edu, tigran.gevorgyan@downstate.edu, douglas.pfeil@downstate.edu, daniel.lee@downstate.edu, randall.barbour@downstate.edu

Abstract: An anatomical atlas-based method for rhesus monkey brain imaging is presented. Numerical simulation, phantom experiment, and animal studies show that the method is computation-efficient in the generation and registration of 3D image findings.

OCIS codes: (100.3010) Image reconstruction techniques; (100.6890) Three-dimensional image processing

1. Introduction

Objective mapping of image findings to the underlying anatomy is becoming an essential capability for functional neuroimaging. In the case of Diffuse Optical Tomography (DOT), complicating the goal of mapping activation findings to brain anatomy is the need for a representative altas that can support the flexible generation of the required image operators for any selected optode arrangement. To facilitate accurate generation and mapping of DOT findings, we have developed an anatomical atlas-based method for DOT human brain imaging. In this report we extend this computation-efficient method to imaging studies of the brain of a Rhesus macaque. A hybrid Rhesus monkey brain atlas is generated by the substitution of a population-average MRI-based brain atlas of the rhesus macaque for an individual rhesus monkey whole head MRI scan. Evaluations from numerical simulation, phantom experiment and animal studies have shown that optode location, reconstruction of activation maps and mapping to the hybrid brain atlas can be made with high fidelity.

2. Methods

For accurate generation and mapping of DOT findings, we have developed an anatomical atlas-based approach for human brain imaging [1,2]. One of the key elements of the method is the established MR-based FEM model library that contains FEM meshes from a selected MR atlas that has been segmented according to different tissue types and the pre-calculated image generators. Using synthetic data, we examined the accuracy by which image finding are mapped to the correct brain structures and subsequently are mapped to an individual's MR image [2]. In this report we extend the atlas-based method to imaging of the Rhesus monkey brain with DOT.

2.1 Generation of Hybrid Rhesus Brain Atlas: To minimize subject bias, a hybrid brain atlas was generated by substitution of a population-averaged MRI-based brain atlas for the Rhesus macaque (112 monkeys: 80 males, 32 females available from the literature [3]), for that of an individual monkey, (healthy, young male), as shown in Fig.1.

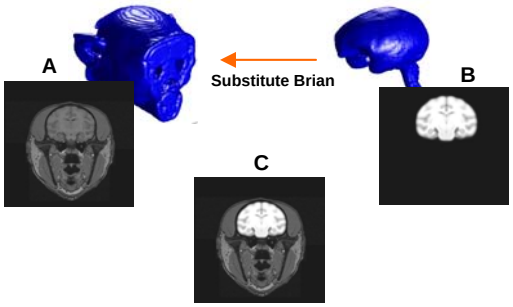

Figure 1. Hybrid brain atlas. (A) individual monkey head; (B) group averaged monkey brain; (c) hybrid monkey atlas.

2.2 FEM Mesh and Image Generator: The hybrid map is segmented into into six main classes including skin, muscle, skull, cerebrospinal fluid, gray matter, and white matter for the generation of 3D finite element method (FEM) mesh, and the image generators are computed by numerically solving photon diffusion equation for assigned tissue coefficients. Fig.2 shows the segmented FEM mesh and a FEM model with 64 sources and 64 detectors.

2.3 Image Reconstruction: 3D images of the Hb signal were reconstructed by using the normalized difference method [4]. This method solves a modified linear perturbation equation that is robust to many of the uncertainties common to experimental studies including uncertainties associated with the initial guess, also known as the reference medium. Use of the linear approximation makes real-time 3D imaging feasible.

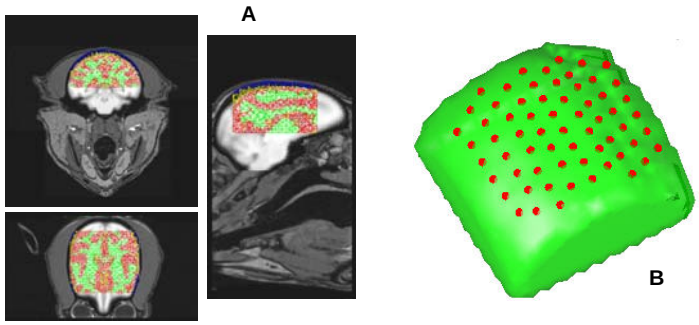

Figure 2. (A) Segmented FEM mesh of an optical imaging region; (B) An FEM model with 64 sources and 64 detectors.

3. Results and Conclusions

Qualitative and quantitative assessments of the fidelity of our method are presented in this section. Shown in Figure 3 is an example of our method applied to simulated data. Here an inclusion having a diameter of 1.0 cm was embedded to a mean depth of 1.2 cm and centrally located with respect to the position of a 30x30 source/detector array. The assigned absorption coefficent value (0.12 cm^{-1}) was twice that of the background; $\mu_{s'}$ = 10 cm^{-1}. To mimic the real experimental data, 2% Gaussian noise was added to simulated detector readings. Fig.3A shows the source/detector array and the inclusion position; Figs.3B and 3C are the inclusion positions and the reconstructed images in the axial, coronal and sagittal views (left to right), respectively. Careful inspection shows that the bias between the inclusion center and reconstructed image center is less than 2.5 mm.

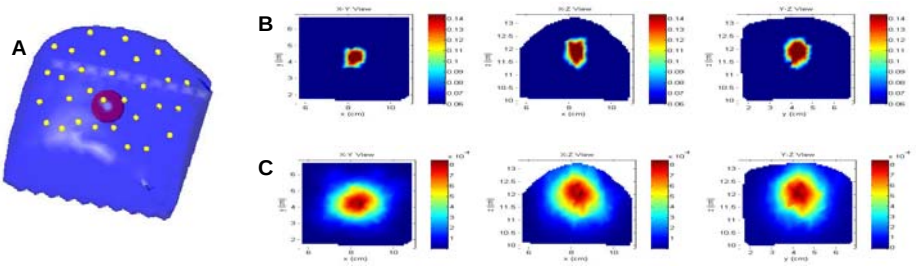

Figure 3. (A) 30x30 Source/detector array and inclusion; (B) Inclusion positions; (C) Reconstructed images.

The reconstructed DOT images from phantom experiment data are presented in Fig.4. In this experiment a solid-state monkey phantom [5] containing a programmable 1x1x0.2 (cm) electrochromic (EC) cell, embedded in left posterior brain at a depth of 1 cm below the surface was used to mimic a spatiotemporal hemodynamic pattern of interest. Shown in Fig.4A are reconstructed total hemoglohin maps, where the location of EC cell is accurately recovered. The reconstructed signal and its FFTs at cell's position are shown in Figs.4B and 4C illustrating excellent recovery of induced signal (1 Hz).

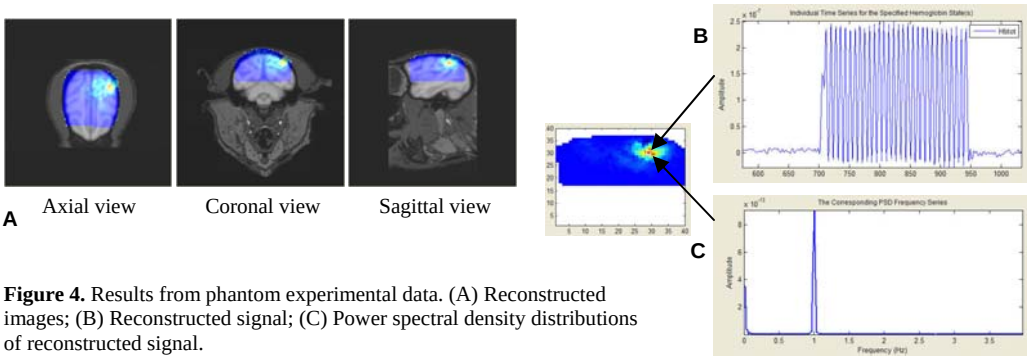

Figure 4. Results from phantom experimental data. (A) Reconstructed images; (B) Reconstructed signal; (C) Power spectral density distributions of reconstructed signal.

Fig.5 shows the results from animal experimental data [6]. In the experiment, macaques were monitored using CW-NIRS DOT imager with probes placed on the exposed skull in the mid frontal-parietal region, and an acute stroke and subarachnoid bleeding was induced via occlusion of the internal carotid and middle cerebral arteries. Post-surgical CT-scan, MRI and brain histopathology revealed concurrence between subarachnoid bleeding, cortical infarction, interventional procedures (contrast, vasodilator injection) and NIRS findings.

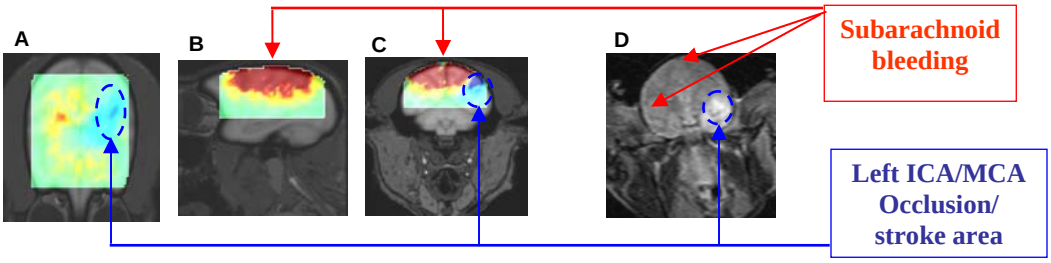

Figure 5. Results from animal experimental data. (A)-(C) Reconstructed total hemoglobin images; (D) MRI at the end of the experiment showing actual stroke area.

In summary, we have developed an anatomical atlas-based method for generation and anatomical mapping of 3D DOT monkey brain image findings. As confirmed by numerical simulations, phantom and animal experimental data, our method is computation-efficient and is able to carry out anatomical mappings with high spatial and temporal accuracy. The reported capabilities have been integrated into our NAVI computing environment [7] to support model-based fNIRS reconstruction and generation of MR-based montages.

4. References

[1] Y. Xu, Y. Pei, and R.L. Barbour, "An anatomical atlas-based method for efficient generation and registration of 3D DOT image findings," Paper NIH01-101 at The Inter-Institute Workshop on Optical Diagnostic and Biophotonic Methods from Bench to Bedside (Bethesda, MD, October 1-2, 2009).

[2] Y. Xu, Y. Pei, and R.L. Barbour, "An anatomical atlas-based method for fNIRS tomography," Poster 864 MT-PM at the Meeting for Human Brain Mapping (Barcelona, Spain, June 6-10, 2010).

[3] Donald G. McLaren, Kristopher J. Kosmatka, et. al., "A population-average MRI-based atlas collection of the rhesus macaque", NeuroImage **45**, pp. 52–59(2009).

[4] Y. Pei, H.L. Graber, and R.L. Barbour (2001), 'Influence of systematic errors in reference states on image quality and on stability of derived information for dc optical imaging', Applied Optics, 40, p. 5755.

[5] R.L. Barbour, R. Ansari, R. Al abdi, et. al., "Validation of near infrared spectroscopic (NIRS) imaging using programmable phantoms," Proceedings of SPIE, Vol. 6870, R.J. Nordstrom, Ed. (2008).

[6] T. Gevorgyan, D.S. Pfeil, H.L. Graber, et. al., " Cerebral monitoring during acute stroke and subarachnoid hemorrhage in the Bonnet Macaques with fNIRS," Paper NIH100-52 at the 7th NIH Inter-Institute Workshop on Optical Diagnostic and Biophotonic Methods from Bench to Bedside (Bethesda, MD, September 15-16, 2011).

[7] Y. Pei, Y. Xu, and R.L. Barbour, "NAVI-SciPort solution: A problem solving environment (PSE) for NIRS data analysis," Poster No. 221 M-AM at Human Brain Mapping 2007 (Chicago, IL, June 10-14, 2007).

This research was support in part by the National Institutes of Health (NIH) under Grants nos. R21NS067278, R42NS050007 and 5R44NS049734; by the Defense Advanced Research Projects Agency; and by the New York State Department of Health.